

**Figure 3. TUNEL-positive crypt cells in the small intestines from KBrO<sub>3</sub>-treated mice.** **A.** The sections stained with TUNEL. The crypts of small intestines from wild type (left) and *Msh2*-deficient (right) mice treated with KBrO<sub>3</sub>. **B.** The number of TUNEL-positive cells in the crypts. The mean numbers of TUNEL-positive cells with standard deviations are indicated by white (wild type mice) and black (homozygous *Msh2*-deficient mice) bars. \*  $p < 0.002$  (Student's *t*-test).

### Analysis of cell death

MMR is involved in the signaling for cell death induced by genotoxic chemicals, such as alkylating agents (19-21). A previous study showed that ES cells carrying disrupted *Msh2* alleles displayed an increased survival following exposure to low-level ionizing radiation compared with wild type ES cells (26). The increased survival could be attributed to a failure of the cells to efficiently execute apoptosis in response to oxidative DNA damage induced by radiation exposure. These findings suggested that MMR is involved in the induction of apoptosis caused by oxidative DNA damage. It has been shown that intestinal cancer originates in the stem cells resided in the bottom of intestinal crypts (37). Thus, in the present study, we analyzed the cell death in the crypts of small intestines from wild type and *Msh2*-deficient

mice treated with KBrO<sub>3</sub> using a TUNEL method. A few TUNEL-positive cells were detected in the crypts of wild type mice, but not in those of *Msh2*-deficient mice (Figure 3A). We counted the TUNEL-positive cells in more than 100 crypts from each genotype of mice. The average numbers of crypts per mouse were as follows: wild type, 21.2 (min 14, max 31) and *Msh2*-deficient, 21.6 (min 17, max 30). We found that  $3.36 \pm 0.96$  (mean  $\pm$  SD) TUNEL-positive cells per crypt were present in wild type mice, while  $0.80 \pm 0.46$  (mean  $\pm$  SD) TUNEL-positive cell per crypt were present in *Msh2*-deficient mice (Figure 3B). This difference was statistically significant ( $p < 0.002$ ; *t*-test).

### Discussion

In the present study, we performed KBrO<sub>3</sub>-induced tumorigenesis experiments using *Msh2*-deficient mice to examine the involvement of mismatch repair (MMR) in the suppression of oxidative stress-induced tumorigenesis. The oral administration of KBrO<sub>3</sub> at a dose of 0.2% in drinking water dramatically increased the formation of intestinal tumors in *Msh2*-deficient mice compared to untreated *Msh2*-deficient mice and treated wild type mice. Thus, we concluded that MMR plays a significant role preventing the intestinal tumorigenesis induced by oxidative stress in mice.

Several lines of evidence suggest that oxidative stress could be generated in the intestines of animals under physiological conditions. For example, it was reported that the incidence of G:C to T:A transversions increases significantly in the intestines of older mice compared with younger mice (38). Because G:C to T:A transversions are mainly caused by 8-oxoG, a major oxidative DNA damage, these observations indicate that the mutations caused by oxidative DNA damage would tend to accumulate in the intestines during the course of aging. Consistent with this notion, defects in MUTYH, the human DNA glycosylase suppressing 8-oxoG-induced mutagenesis, lead to a susceptibility to colorectal cancers with excess G:C to T:A transversions in humans (39). Furthermore, *Mut yh*-deficient mice also show susceptibility to spontaneous and KBrO<sub>3</sub>-induced intestinal adenoma/carcinoma (34). Therefore, based on these previous observations and our present results, it is likely that on a MMR-defective genetic background, oxidative stress generated in the intestine may enhance tumor development, thus leading to HNPCC in humans.

The mutation analyses of the tumor-related gene, *Ctmb1*, revealed that more than 30% of the tumors that developed in KBrO<sub>3</sub>-treated *Msh2*-deficient mice had somatic mutations in the coding region for GSK3 $\beta$  phosphorylation sites. All the mutations detected

were base substitutions; 20 G:C to A:T transitions (74.1%), three A:T to G:C transitions (11.1%), two G:C to T:A transversions and two G:C to C:G transversions (7.4%). These observations are consistent with the results obtained from mutation analyses of the *CTNNB1* gene in cancers from HNPCC patients; 12 reported base substitutions were as follows: TCT to TTT, CCT, or TGT at codon S45; ACC to GCC at codon T41; TCT to TGT at codon S37; GGA to GAA at codon G34; GAC to GGC or TAC at codon D32 (40). The G:C to A:T transition at codon G34 and G:C to C:G transversion at codon S37 were commonly observed in both human and mouse tumors. The difference observed between human and mouse mutation spectra may due to the different nucleotide sequence context in this locus of these two species. The similarity of the mutation types and spectra suggests that the KBrO<sub>3</sub>-treatment of mice may mimic the oxidative stress in human to induce DNA damage in the intestine. We detected only two G:C to T:A transversions, thus suggesting that the DNA repair enzymes, including Ogg1 and Mutyh, may suppress 8-oxoG-related mutagenesis to some extent in KBrO<sub>3</sub>-treated *Msh2*-deficient mice. Besides the one G:C to T:A transversion at the codon for S33, three types of mutations other than the G:C to A:T transition were observed at only the codon for S37; three A:T to G:C transitions, two G:C to C:G transversions, and one G:C to T:A transversion. Because these types of mutations were suppressed by the overexpression of MTH1, which hydrolyzes oxidized purine nucleotide triphosphates, in *MSH2*-deficient human cells (28, 29), the nucleotide sequence context around the codon for S37 might be competent to enhance the incorporation of oxidatively-damaged purine nucleotide triphosphates by DNA polymerase.

MMR factors are well known to be involved in the induction of apoptosis caused by O<sup>6</sup>-methylguanine (O<sup>6</sup>-mG), a type of DNA damage produced by alkylating agents (19-21). O<sup>6</sup>-mG can pair with thymine during DNA replication, forming O<sup>6</sup>-mG:T mispairs. MutSα recognizes this mispair and forms a complex with MutLα and PCNA to induce apoptosis (20). The *Msh2*-deficiency also caused a failure to induce apoptosis effectively in response to oxidative DNA damage (26). Thus, in the present study, we analyzed the cell death of the crypts of small intestines from wild type and *Msh2*-deficient mice treated with KBrO<sub>3</sub> using a TUNEL assay. A larger number of TUNEL-positive cells were observed in the crypts from wild type mice compared with *Msh2*-deficient mice, suggesting that the crypt cells with MMR-deficiencies showed an increased chance of surviving protracted exposure to KBrO<sub>3</sub>. The better survival of MMR-deficient cells with pre-mutagenic

lesions in the genome induced by oxidative stresses may contribute to the increased cancer risk characteristic of the hereditary non-polyposis colorectal cancer syndrome.

In conclusion, we herein demonstrated that oxidative stress enhanced the tumor formation in the small intestines of *Msh2*-deficient mice, thereby providing experimental evidence of the association between oxidative stress and hereditary non-polyposis colorectal cancer caused by MMR-deficiency in humans. We propose that MMR suppresses spontaneous tumorigenesis in the intestines of mammals by simultaneously preventing the occurrence of mutations and the removal of precancerous cells containing pre-mutagenic oxidative lesions in the genome.

## Acknowledgements

We thank Dr. Brian Quinn for comments on the manuscript. We also appreciate the technical support from the Research Support Center, Graduate School of Medical Sciences, Kyushu University. This work was supported by grants from Japan Society for the Promotion of Science, and the Ministry of Health, Labor and Welfare of Japan.

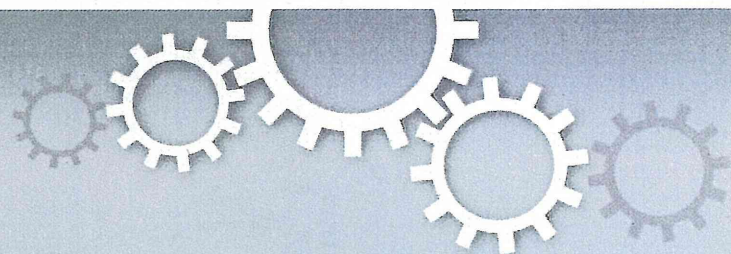
## Competing Interests

The authors have declared that no competing interest exists.

## References

- Ames BN, Shigenaga MK Hagen TM. Oxidants, antioxidants, and the degenerative diseases of aging. *Proc Natl Acad Sci USA*. 1993; 90: 7915-22.
- Gajewski E, Rao G, Nackerdien Z, Dizdaroglu M. Modification of DNA bases in mammalian chromatin by radiation-generated free radicals. *Biochemistry*. 1990; 29: 7876-82.
- Kasai H, Nishimura S. Hydroxylation of deoxyguanosine at the C-8 position by ascorbic acid and other reducing agents. *Nucleic Acids Res*. 1984; 12: 2137-45.
- Fraga CG, Shigenaga MK, Park JW, Degan P, Ames BN. Oxidative damage to DNA during aging: 8-hydroxy-2'-deoxyguanosine in rat organ DNA and urine. *Proc Natl Acad Sci USA*. 1990; 87: 4533-7.
- Shibutani S, Takeshita M, Grollman AP. Insertion of specific bases during DNA synthesis past the oxidation-damaged base 8-oxodG. *Nature*. 1991; 349: 431-4.
- Smith KC. Spontaneous mutagenesis: experimental, genetic and other factors. *Mutat Res*. 1992; 277: 139-162.
- Radicella JP, Dherin C, Desmaze C, Fox MS, Boiteux S. Cloning and characterization of hOGG1, a human homolog of the OGG1 gene of *Saccharomyces cerevisiae*. *Proc Natl Acad Sci USA*. 1997; 94: 8010-5.
- Rosenquist TA, Zharkov DO, Grollman AP. Cloning and characterization of a mammalian 8-oxoguanine DNA glycosylase. *Proc Natl Acad Sci USA*. 1997; 94(14): 7429-34.
- Ohtsubo T, Nishioka K, Imaiso Y, et al. Identification of human MutY homolog (hMYH) as a repair enzyme for 2-hydroxyadenine in DNA and detection of multiple forms of hMYH located in nuclei and mitochondria. *Nucleic Acids Res*. 2000; 28:1355-64.
- Shinmura K, Yamaguchi S, Saitoh T, et al. Adenine excisional repair function of MYH protein on the adenine:8-hydroxyguanine base pair in double-stranded DNA. *Nucleic Acids Res*. 2000; 28: 4912-8.
- Slupska MM, Luther WM, Chiang JH, Yang H, Miller JH. Functional expression of hMYH, a human homolog of the *Escherichia coli* MutY protein. *J Bacteriol*. 1999; 181: 6210-3.
- Takao M, Zhang QM, Yonei S, Yasui A. Differential subcellular localization of human MutY homolog (hMYH) and the functional activity of adenine:8-oxoguanine DNA glycosylase. *Nucleic Acids Res*. 1999; 27: 3638-44.

13. Mo JY, Maki H, Sekiguchi M. Hydrolytic elimination of a mutagenic nucleotide, 8-oxodGTP, by human 18-kilodalton protein: sanitization of nucleotide pool. *Proc Natl Acad Sci USA*. 1992; 89: 11021-5.
14. Sakumi K, Furuichi M, Tsuzuki T, et al. Cloning and expression of cDNA for a human enzyme that hydrolyzes 8-oxo-dGTP, a mutagenic substrate for DNA synthesis. *J Biol Chem*. 1993; 268: 23524-30.
15. Fujikawa K, Kamiya H, Yakushiji H, et al. The oxidized forms of dATP are substrates for the human MutT homologue, the hMTH1 protein. *J Biol Chem*. 1999; 274: 18201-5.
16. Fujikawa K, Kamiya H, Yakushiji H, Nakabeppu Y, Kasai H. Human MTH1 protein hydrolyzes the oxidized ribonucleotide, 2-hydroxy-ATP. *Nucleic Acids Res*. 2001; 29: 449-54.
17. Bjelland S, Seeberg E. Mutagenicity, toxicity and repair of DNA base damage induced by oxidation. *Mutat Res*. 2003; 531: 37-80.
18. Iyer RR, Pluciennik A, Burdett V, Modrich PL. DNA mismatch repair: functions and mechanisms. *Chem. Rev*. 2006; 106: 302-23.
19. Stojic L, Brun R, Jiricny J. Mismatch repair and DNA damage signalling. *DNA Repair (Amst)*. 2004; 3: 1091-1101.
20. Hidaka M, Takagi Y, Takano TY, Sekiguchi M. PCNA-MutS $\alpha$ -mediated binding of MutL $\alpha$  to replicative DNA with mismatched bases to induce apoptosis in human cells. *Nucleic Acids Res*. 2005; 33: 5703-12.
21. Jiricny, J. The multifaceted mismatch-repair system. *Nat Rev Mol Cell Biol*. 2006; 7: 335-46.
22. Fishel R, Lescoe MK, Rao MR, et al. The human mutator gene homolog MSH2 and its association with hereditary nonpolyposis colon cancer. *Cell*. 1993; 75: 1027-38.
23. Leach FS, Nicolaides NC, Papadopoulos N, et al. Mutations of a MutS homologue in hereditary nonpolyposis colorectal cancer. *Cell*. 1993; 75: 1215-25.
24. Bronnner CE, Baker SM, Morrison PT, et al. Mutation in the DNA mismatch repair gene homologue hMLH1 is associated with hereditary non-polyposis colon cancer. *Nature*. 1994; 368: 258-61.
25. Papadopoulos N, Nicolaides NC, Wei YF, et al. Mutation of a MutL homologue in hereditary colon cancer. *Science*. 1994; 263: 1625-9.
26. DeWeese TL, Shipman JM, Larrier NA, et al. Mouse embryonic stem cells carrying one or two defective Msh2 alleles respond abnormally to oxidative stress inflicted by low-level radiation. *Proc. Natl. Acad. Sci. USA*. 1998; 95: 11915-20.
27. Egashira A, Yamauchi K, Yoshiyama K, et al. Mutational specificity of mice defective in the MTH1 and/or the MSH2 genes. *DNA Repair (Amst)*. 2002; 1: 881-93.
28. Colussi C, Parlanti E, Degan P, et al. The mammalian mismatch repair pathway removes DNA 8-oxodGMP incorporated from the oxidized dNTP pool. *Current Biol*. 2002; 12: 912-8.
29. Russo MT, Blasi MF, Chiera F, et al. The oxidized deoxynucleoside triphosphate pool is a significant contributor to genetic instability in mismatch repair-deficient cells. *Mol Cell Biol*. 2004; 24: 465-74.
30. Kasai H, Nishimura S, Kurokawa Y, Hayashi Y. Oral administration of the renal carcinogen, potassium bromate, specifically produces 8-hydroxydeoxyguanosine in rat target organ DNA. *Carcinogenesis*. 1987; 8: 1959-1.
31. DeAngelo AB, George MH, Kilburn SR, Moore TM, Wolf DC. Carcinogenicity of potassium bromate administered in the drinking water to male B6C3F1 mice and F344/N rats. *Toxicol Pathol*. 1998; 26: 587-94.
32. Kurokawa Y, Maekawa A, Takahashi M, Hayashi Y. Toxicity and carcinogenicity of potassium bromate—a new renal carcinogen. *Environ Health Perspect*. 1990; 87: 309-35.
33. Kawanishi S, Murata M. Mechanism of DNA damage induced by bromate differs from general types of oxidative stress. *Toxicology*. 2006; 221: 172-8.
34. Sakamoto K, Tominaga Y, Yamauchi K, et al. MUTYH-null mice are susceptible to spontaneous and oxidative stress-induced intestinal tumorigenesis. *Cancer Res*. 2007; 67: 6599-604.
35. Schlemper RJ, Riddell RH, Kato Y, et al. The Vienna classification of gastrointestinal epithelial neoplasia. *Gut*. 2000; 47: 251-5.
36. Polakis P. Wnt signaling and cancer. *Genes Dev*. 2000; 14: 1837-51.
37. Barker N, Ridgway RA, van Es JH, et al. Crypt stem cells as the cells-of-origin of intestinal cancer. *Nature*. 2009; 457: 608-11.
38. Dolle ME, Snyder WK, Gossen JA, Lohman PH, Vijg J. Distinct spectra of somatic mutations accumulated with age in mouse heart and small intestine. *Proc Natl Acad Sci USA*. 2000; 97: 8403-8.
39. Al-Tassan N, Chmiel NH, Maynard J, et al. Inherited variants of MYH associated with somatic G:C→T:A mutations in colorectal tumors. *Nat Genet*. 2002; 30: 227-32.
40. Miyaki M, Iijima T, Kimura J, et al. Frequent mutation of beta-catenin and APC genes in primary colorectal tumors from patients with hereditary nonpolyposis colorectal cancer. *Cancer Res*. 1999; 59: 4506-9.



## OPEN

8-oxoguanine causes spontaneous *de novo* germline mutations in mice

## SUBJECT AREAS:

EVOLUTIONARY  
BIOLOGY  
MUTATIONMizuki Ohno<sup>1</sup>, Kunihiko Sakumi<sup>2,3</sup>, Ryutaro Fukumura<sup>4</sup>, Masato Furuichi<sup>5</sup>, Yuki Iwasaki<sup>6,7</sup>, Masaaki Hokama<sup>2</sup>, Toshimichi Ikemura<sup>6</sup>, Teruhisa Tsuzuki<sup>1</sup>, Yoichi Gondo<sup>4</sup> & Yusaku Nakabeppu<sup>2,3</sup>

<sup>1</sup>Department of Medical Biophysics and Radiation Biology, Faculty of Medical Sciences, Kyushu University, Fukuoka 812-8582, Japan, <sup>2</sup>Division of Neurofunctional Genomics, Department of Immunobiology and Neuroscience, Medical Institute of Bioregulation, Kyushu University, Fukuoka 812-8582, Japan, <sup>3</sup>Research Center for Nucleotide Pool, Kyushu University, Fukuoka 812-8582, Japan, <sup>4</sup>Mutagenesis and Genomics Team, RIKEN BioResource Center, Tsukuba 305-0074, Japan, <sup>5</sup>Radioisotope Center, Kyushu University, Fukuoka 812-8582, Japan, <sup>6</sup>Department of Computer Bioscience, Nagahama Institute of Bio-Science and Technology, Nagahama 526-0829, Japan, <sup>7</sup>Research Fellow of the Japan Society for the Promotion of Science.

Received  
8 January 2014Accepted  
28 March 2014Published  
15 April 2014

Correspondence and requests for materials should be addressed to K.S. (sakumi@bioreg.kyushu-u.ac.jp)

Spontaneous germline mutations generate genetic diversity in populations of sexually reproductive organisms, and are thus regarded as a driving force of evolution. However, the cause and mechanism remain unclear. 8-oxoguanine (8-oxoG) is a candidate molecule that causes germline mutations, because it makes DNA more prone to mutation and is constantly generated by reactive oxygen species *in vivo*. We show here that endogenous 8-oxoG caused *de novo* spontaneous and heritable G to T mutations in mice, which occurred at different stages in the germ cell lineage and were distributed throughout the chromosomes. Using exome analyses covering 40.9 Mb of mouse transcribed regions, we found increased frequencies of G to T mutations at a rate of  $2 \times 10^{-7}$  mutations/base/generation in offspring of *Mth1/Ogg1/Mutyh* triple knockout (TOY-KO) mice, which accumulate 8-oxoG in the nuclear DNA of gonadal cells. The roles of MTH1, OGG1, and MUTYH are specific for the prevention of 8-oxoG-induced mutation, and 99% of the mutations observed in TOY-KO mice were G to T transversions caused by 8-oxoG; therefore, we concluded that 8-oxoG is a causative molecule for spontaneous and inheritable mutations of the germ lineage cells.

Evolution requires *de novo* germline mutations that are newly generated in germ lineage cells and inheritable to the offspring. It is evident that germline mutations occur, because sporadic and deleterious mutations that cannot be transmitted to offspring continuously appear in human populations<sup>1–4</sup>. The human *de novo* germline mutation rate is estimated to be  $1.20 \times 10^{-8}$ /nucleotide/generation<sup>1</sup>. However, the cause and mechanism of mutations in the germ cell lineage remain unclear. We hypothesized that the cause of these mutations would be endogenously and spontaneously generated and remain in the germ cell lineage. 8-oxoG is one of the candidate molecules for causing germline mutation, because it is endogenously generated by reactive oxygen species (ROS) derived from cellular respiration, constitutively exists in DNA<sup>5</sup> and is known to cause G to T and A to C transversion mutations by the ability to pair with A as well as C during DNA replication<sup>6–8</sup>.

Mammals possess three enzymes to avoid 8-oxoG-induced mutations. MTH1 (*mutT* homologue 1, NUDT1) degrades 8-oxodGTP in the nucleotide pool to prevent its incorporation into DNA<sup>9</sup>. OGG1 (8-oxoG DNA glycosylase) excises 8-oxoG from DNA<sup>10,11</sup>, and MUTYH (*mutY* homologue, adenine DNA glycosylase) removes adenine misincorporated opposite 8-oxoG in DNA<sup>12</sup>. We and other groups have reported that mice deficient in these enzymes are prone to developing cancer, indicating a mutator phenotype in somatic cells<sup>13–16</sup>. MUTYH is also responsible for MUTYH-associated polyposis in humans<sup>17</sup>.

To evaluate the contribution of 8-oxoG to *de novo* germline mutation, we established the *Mth1/Ogg1/Mutyh* triple knockout (TOY-KO) mice, in which unrepaired endogenous 8-oxoG accumulates in the genome DNA. In this paper, using the TOY-KO mice, we showed that 8-oxoG causes G to T mutations in germ lineage cells (Supplementary Fig. S1 online).

## Results

**Spontaneous mutations increased in *Mth1*<sup>−/−</sup>/*Ogg1*<sup>−/−</sup>/*Mutyh*<sup>−/−</sup> (TOY-KO) mice.** To evaluate the contribution of 8-oxoG to *de novo* germline mutation, we established the TOY-KO mouse in the C57BL/6J background (>N16). TOY-KO mice are viable and fertile, although increased amounts of 8-oxoG accumulated in various tissues, including the gonads (Fig. 1a). Moreover, TOY-KO mice had a shorter lifespan (Fig. 1b) and developed various types of tumors (Fig. 1c). We maintained the TOY-KO mouse line originating from one pair

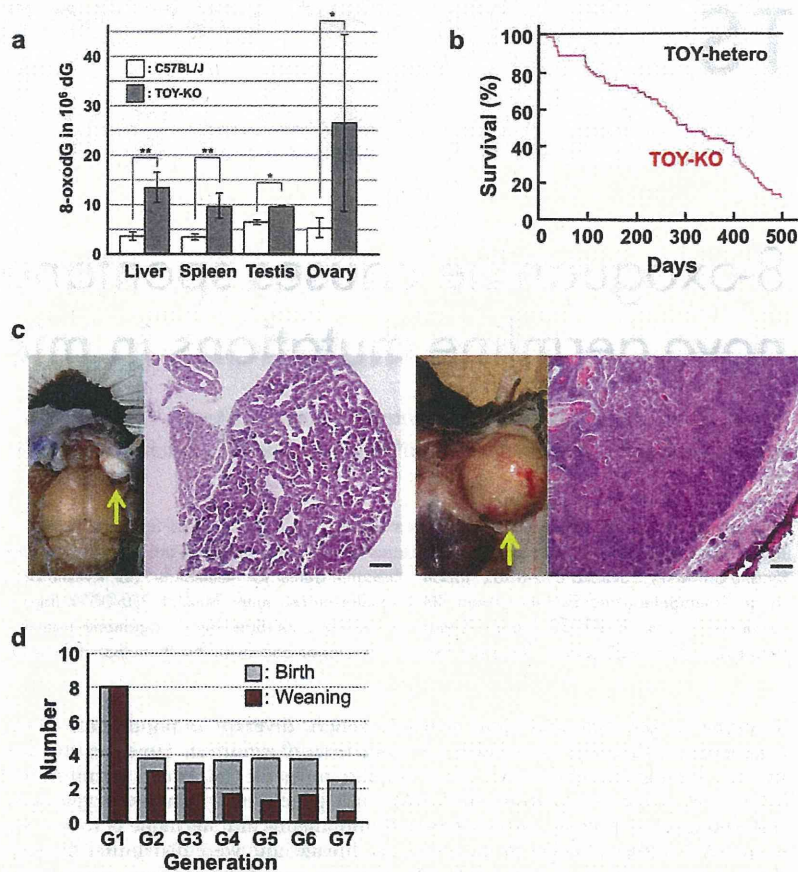


**Figure 1 | Phenotype of TOY-KO mice.** (a) Accumulation of 8-oxodG in TOY-KO mouse tissues. LC-MS/MS was used to determine the amount of 8-oxodG<sup>29</sup>. Data are presented as the means  $\pm$  SD. Wilcoxon tests were used to analyze differences between TOY-KO (gray) and C57BL/6J:Jcl (open) mouse tissues (\*  $P < 0.05$ ; \*\*  $P < 0.001$ ). (b) Survival of TOY-KO mice. The survival curve of TOY-KO mice ( $n = 56$ , indicated in red) was compared with that of *Mth1*<sup>+/-</sup>/*Ogg1*<sup>+/-</sup>/*Mutyh*<sup>+/-</sup> (TOY-hetero) mice ( $n = 14$ , indicated in black). (c) A Harderian gland tumor (left) and a trichoepithelioma (right) observed in a TOY-KO mice (indicated by arrows). Hematoxylin and eosin staining of each tumor is shown. Scale bars, 200  $\mu$ m. (d) Numbers of newborn and weaned mice. Gray and red bars indicate the numbers of newborn and weaned mice in each generation of TOY-KO mice, respectively.

(G1) to the 8th generation (G8) by intragenerational mating (Supplementary Fig. S2 online). More than 35% of TOY-KO mice carried macroscopically distinguishable tumors (Supplementary Fig. S2 online). As the generations increased, it became difficult to obtain mice for breeding because of the decreased number of weaned mice (Fig. 1d). Several phenotypic variations were found among the progeny, such as hydrocephalus, belly white spot and anophthalmia (Supplementary Fig. S2 online). In cases of hydrocephalus and white spot, the traits were transmitted to the next generation in an autosomal dominant fashion with incomplete penetrance (Fig. 2, Supplementary Fig. S2 online). These features indicate that heritable mutations could arise in the TOY-KO mice.

To detect mutations that occur in the germ cell lineage and are transmitted across generations of TOY-KO mice, we performed whole exome sequencing analysis (Fig. 3a). We searched for different sequences between the C57BL/6J mouse reference genome (MGSCv37) and TOY-KO mice that belonged to the most advanced generation of each branch of the pedigree (TOY365F, TOY609F and TOY450F, shown in Fig. 3b). No sequencing reads corresponding to parts of the wild-type reference sequences of targeted *Mutyh*, *Mth1*, and *Ogg1* loci were obtained in chromosomes 4, 5, and 6, respectively (Supplementary Fig. S3 online), which confirmed that the TOY-KO mouse was indeed deficient for the three genes, and validated our exome analysis. By analyzing the exome covering 40.9 Mb of mouse transcribed sequences, which included 19,427

genes from 17 chromosomes, excluding chromosomes 4, 5, and 6 from the analysis to avoid ambiguity, we identified 262 base substitution mutations (Fig. 3c, Supplementary Table S1 online, Supplementary Data S1 online). No insertion/deletion mutations were detected in this analysis.

**Identification of mutation origin mice.** The 262 mutations detected in TOY365F, TOY609F and TOY450F had occurred in one of the mice in the 8-generations of the pedigree (Fig. 3b); therefore, we determined the mutation origin mouse that initially possessed the mutated allele in its tail DNA. We traced each mutation on the pedigree by determining the sequences of all mutated alleles in 35 TOY-KO mice shown in the pedigree (Fig. 3b), using MassArray or Sanger's sequencing, and identified the origin of each *de novo* mutation. The results of the sequencing are summarized in Supplementary Data S1 online with annotations. Among them, we considered that 247 mutations found in G2–G8 mice had spontaneously occurred in the germ cell lineage of TOY-KO mice, because these mutated alleles were derived from gametes of their parent mice (G1–G7) or were generated during early development of the mice (G2–G8). The spectrum of germline mutation observed in TOY-KO mice indicated a distinct feature: 99% (244/247) of the mutations were G to T transversions (Table 1). G to T mutations had specifically increased in TOY-KO mice lacking the ability to avoid 8-oxoG-induced mutations; therefore, we concluded that 8-oxoG is a causative

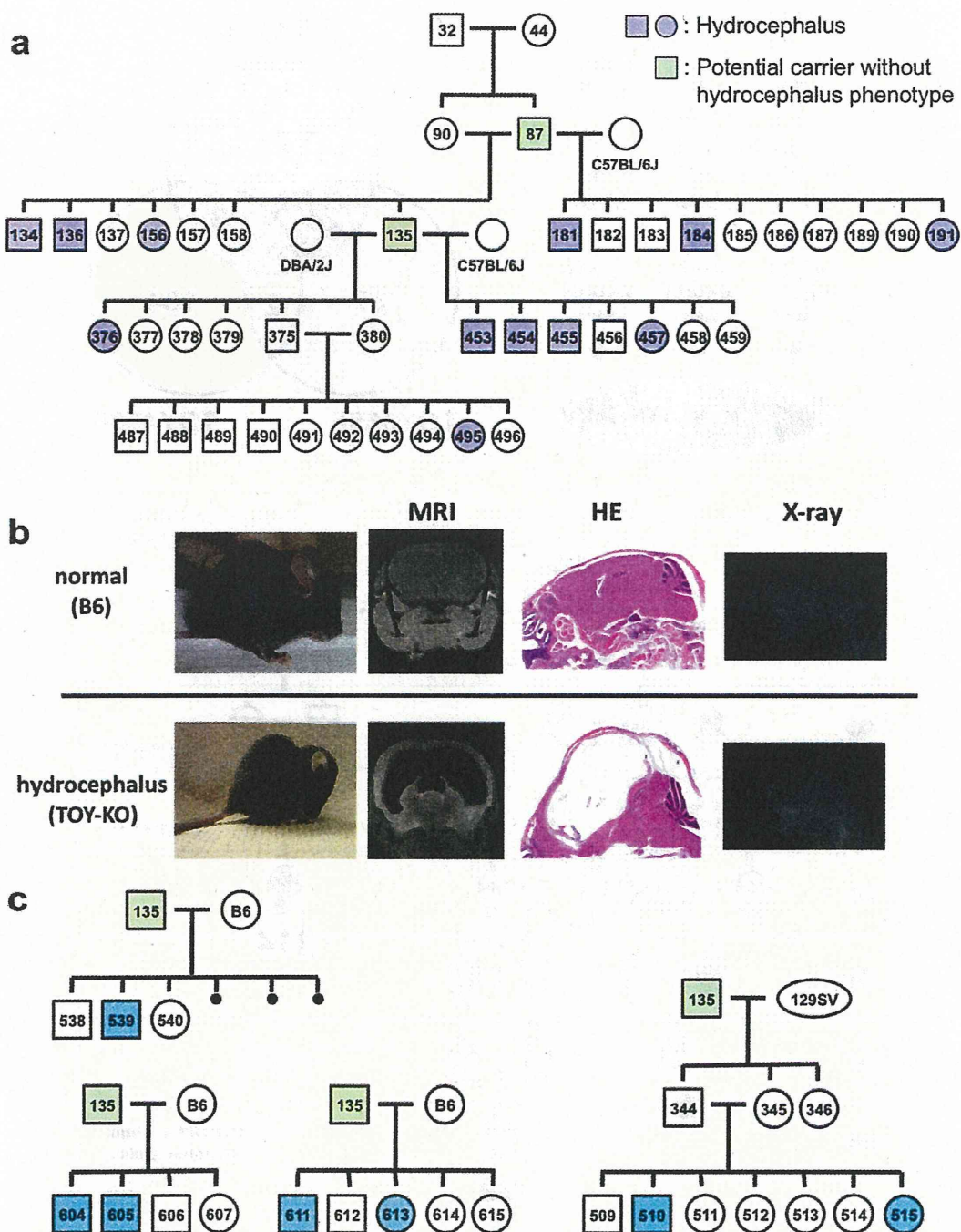


**Figure 2 | Phenotypic variations observed in the progeny of TOY-KO mice.** (a) The hydrocephalus trait was transmitted to the next generation in the TOY-KO pedigree. A hematoxylin/eosin-stained section showing the typical features of the hydrocephalus trait. Blue indicates a mouse with hydrocephalus, and green indicates a mouse carrying the causative mutation without the hydrocephalus phenotype (also shown in Supplementary Fig. S2 online). (b) Hydrocephalus. MRI, hematoxylin/eosin staining and X-ray images of normal (C57BL/6J) and hydrocephalus TOY-KO mice are shown in the upper panel. MRI images were obtained using an MRI mini SA (DS Pharma Biomedical Co. Ltd., Suita, Japan). X-ray images were obtained using a  $\mu$ FX-1000 (Fuji Photo File Co. Ltd.). (c) Pedigrees of the TOY-KO mouse mated with C57BL/6J (shown as B6) and 129Sv mice are shown in the lower panel. Blue indicates a mouse with hydrocephalus, and green indicates a mouse carrying the causative mutation without the hydrocephalus phenotype.

molecule for spontaneous G to T mutation in the mouse germ cell lineage. These mutations arose in all progeny of each generation and in all chromosomes that we analyzed (Figs. 4 and 5a). The mutations ranged from synonymous substitutions to harmful mutations, such as a gain of a stop codon in the *Ttn* gene responsible for human hypertrophic cardiomyopathy<sup>18</sup> (Supplementary Data S1 online).

By analyzing the position of the mutated G in di- and tri-nucleotide sequences, we found that G to T mutations occurred more often at GpC sites than at CpG sites, and tended to occur at tri-nucleotides, which are typical sequences found in triplet repeat expansion disorders (Fig. 5b, c), such as CAG (Huntington's disease), CTG (Myotonic dystrophy) and GAA (Friedreich ataxia)<sup>19</sup>. It is probable

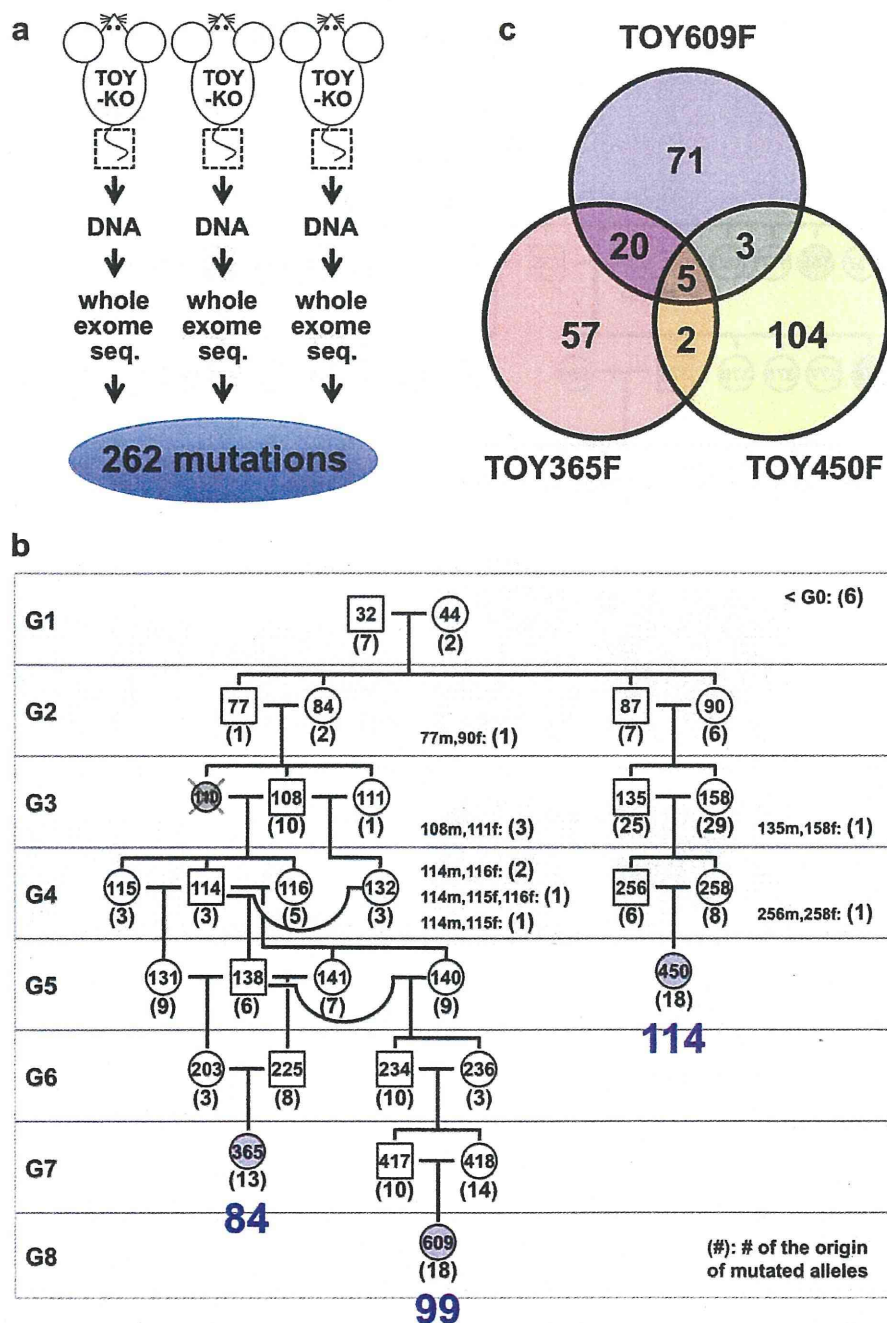


**Figure 3 | Identification of *de novo* germline mutations in TOY-KO mice.** (a) Scheme for screening of germline mutations. (b) Pedigree of TOY-KO mice used for germline mutation analysis. TOY365F, TOY609F and TOY450F were used to identify *de novo* germline mutations. Blue numbers, 84, 98, and 114, indicate the number of mutations detected in TOY365F, TOY609F and TOY450F, respectively. Numbers in parentheses indicate the number of original mutations in each generation, which were found in tail DNA for the first time in the pedigree. The DNA of TOY110F was unavailable; therefore, the mouse was excluded from the analysis. (c) The numbers of base substitution mutations found in TOY365F, TOY609F and TOY450F.

that uneven distribution of mutable 8-oxoG is reflected by the tendency for DNA oxidation, or by the site preference of DNA polymerases in incorporating 8-oxodGTP. We also detected two G to A and one A to G transition mutations that were classified as synonymous coding or intronic mutations (Table 1, Supplementary Data S1 online).

***De novo* germline mutation rate of TOY-KO mouse.** The detected mutations accumulated in TOY365F, TOY450F and TOY609F

contained parts of the mutations that had occurred in the germ cells of the ancestral mice, because only half of the chromosomes derived from the father and mother had transmitted to the offspring via gametogenesis and fertilization in each generation. The numbers of newly arisen mutations detected only in TOY365F, TOY450F and TOY609F were 13, 18 and 18, respectively (Fig. 3b). Therefore, the *de novo* germline mutation rate was calculated to be  $2.0 \times 10^{-7}$ /base/generation ( $13 + 18 + 18/3/40.9 \text{ Mb} \times 2/\text{generation}$ ). This mutation rate is 18-fold higher than the basal level,  $1.1 \times$



	All	G2–G8
G:C to A:T	7	2
A:T to G:C	2	1
G:C to T:A	252	244
A:T to C:G	1	0
G:C to C:G	0	0
A:T to T:A	0	0
total	262	247

Mutations detected in the 40.9 Mb exome sequences of TOY365F, TOY450F, and TOY609F (Fig. 3a) were classified into mutation types. The mutations observed in G2–G8 mice (Fig. 3b) were considered as mutations that occurred in the TOY-KO germ cell lineage.

$10^{-8}$  mutations/base/generation, calculated from the specific locus test in mice<sup>20</sup>. For human trio analysis<sup>1</sup>, the germline mutation rate was calculated to be  $1.2 \times 10^{-8}$  mutation/base/generation, and the G to T transversion mutation was observed in about 9% of all mutations. These results indicated that an approximately 200-fold increase in G to T transversion mutations occurred in the TOY-KO mice. No G to A transition mutations occurred in TOY365F, TOY450F, and TOY609F (totaling 245.4 Mb); therefore, the background mutation level of the TOY-KO mouse was estimated to be less than  $4.1 \times 10^{-9}$  G to A transition mutation/base/generation. This background mutation level is not high compared with that in humans ( $4.9 \times 10^{-9}$  G to A transition mutation/base/generation)<sup>1</sup>.

**Fates of *de novo* germline mutations.** By following up the mutated alleles in the pedigree, we observed the fates of the *de novo* mutations, in which some were fixed and others were eliminated in later generations. As shown in Fig. 6, for example, mutation #187 initially appeared in TOY108M (G3) as a heterozygous allele, indicating that the mutation probably occurred in the germ cell lineage of the parents, either TOY77M or TOY84F, and was transmitted to the progeny. At G5, it became homozygous in TOY138M and TOY131F, and thus fixed in the progeny. Conversely, in another branch, the mutant allele was not transmitted to the offspring and eventually disappeared. These behaviors of the mutated allele represent the appearance, transmission, fixation and disappearance of a spontaneous mutation, which are the typical fates of a novel mutation in the evolutionary process.

## Discussion

Little research has been performed to identify the causative molecule of spontaneous germline mutations because it is a rare event. We considered that the causative molecule must possess certain features that make DNA more prone to mutation, be generated endogenously and spontaneously and remain in the germ cell lineage. In 2006, we reported that endogenous 8-oxoG is distributed in the genome of human lymphocytes in the steady state<sup>5</sup>. We hypothesized that 8-oxoG also exists in the genome of germ lineage cells, and is responsible for spontaneous *de novo* germline mutations, because 8-oxoG is endogenously generated by ROS derived from cellular respiration, and is known to cause transversion mutations. By disruption of the

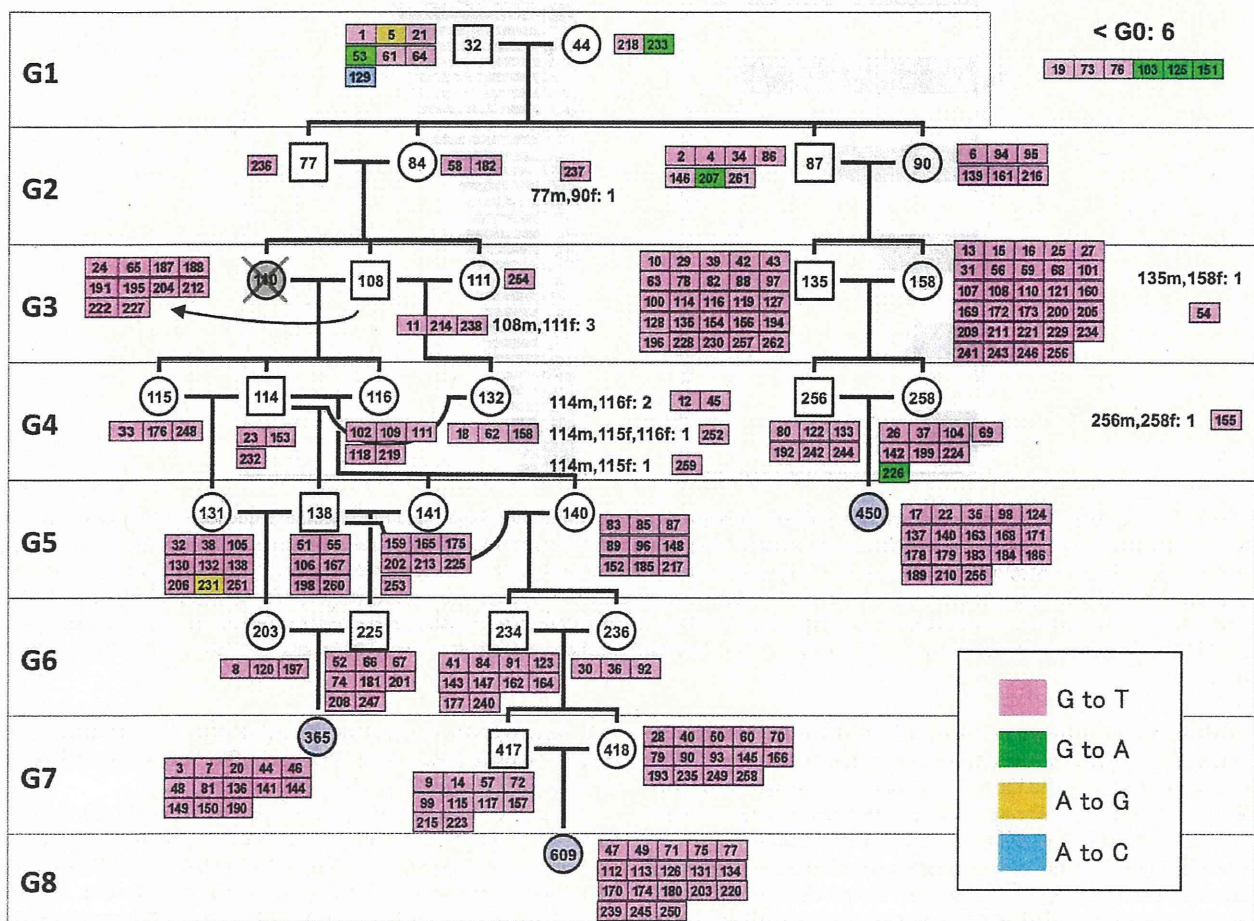


**Figure 4 | Heritable mutations mapped in the pedigree of TOY-KO mice.** The number in each box indicates the mutation ID number shown in Supplementary Data S1 online, and the color indicates the mutation category.



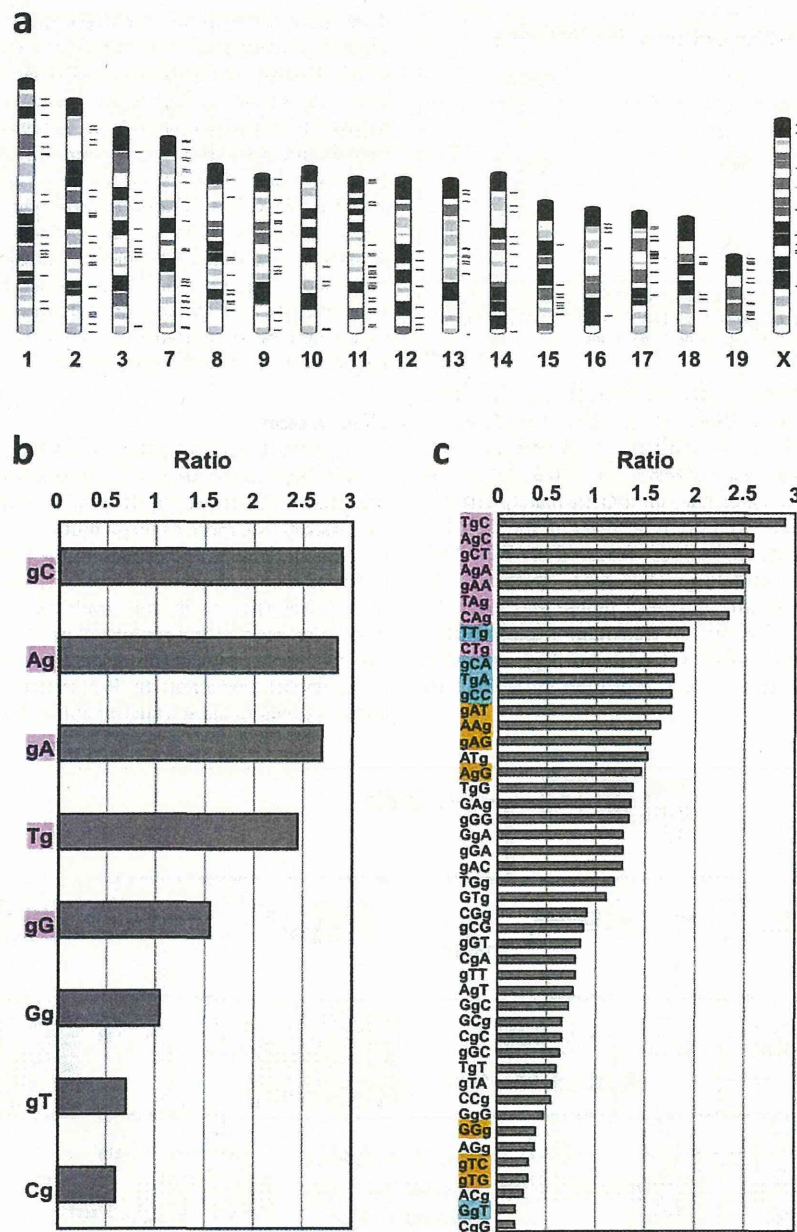


**Figure 5 | Genome-wide distribution of mutations and site preferences of G to T mutations in di- and trinucleotide sequences. (a)** Mutations detected in G2–G8 were mapped on a mouse G-band ideogram using Ideographica (<http://www.ncrna.org/idiographica/>). Each black transverse line on the right side of the chromosome represents a mutation site. **(b)** Site preferences of G to T mutations in di-nucleotide sequences. The plots represent the relative ratio of the actual value of detected mutations (G to T mutations in G2–G8) in each di-nucleotide to its occurrence level in the analyzed exome sequences. ‘g’ indicates the position of a mutated guanine. **(c)** Site preferences of G to T mutations in tri-nucleotides. For each nucleotide sequence, a chi square test (detected vs. expected) was performed, and the colored sequences indicate a significant difference:  $P < 0.001$  (pink),  $P < 0.01$  (blue), and  $P < 0.05$  (orange).

8-oxoG exclusion system in mice, we detected increased spontaneous accumulation of germline mutations during the generations. These mutations were distributed throughout the chromosomes and inheritable to offspring across the generations, leading to an expansion of genetic diversity as well as disease-associated mutations.

The effects of 8-oxoG on spontaneous germline mutations were apparent in the TOY-KO mice. However, the production of 8-oxoG is dependent on the oxidation of guanine nucleotides, which occurs even in the wild-type cells independently of MTH1, OGG1 and MUTYH activities. It is likely that 8-oxoG universally causes *de novo*

G-T transversion mutations, including germline mutations, although most of these mutations are efficiently prevented by the MTH1, OGG1 and MUTYH enzyme system.

When did the germline mutations occur? It is difficult to determine the timing of the occurrence of a mutation in the germ cell lineage; however, some examples were obtained that allowed us to speculate on the timing of mutations in our experiment. *De novo* mutations occur either in the germ cell lineage of the previous generation or during the very early developmental stage of the mutant mouse (Fig. 7). In eleven cases among 247 mutations, the mutations

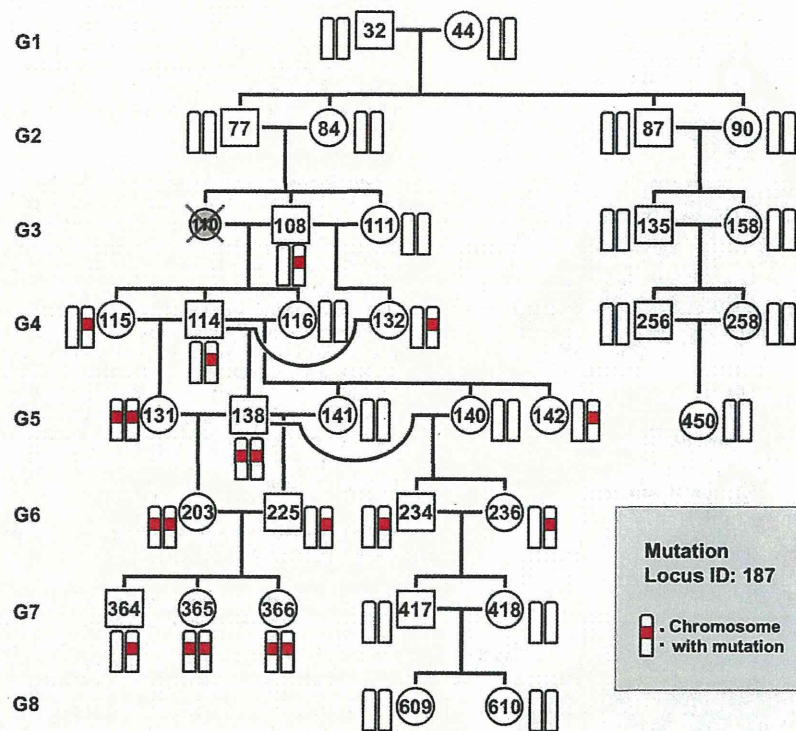


**Figure 6 | Fate of a germline mutation.** Mutation #187 (Ch. 15) was chosen to show the fate of a mutation generated in TOY-KO mice through the generations. This mutation initially appeared in TOY108M (G3) as a heterozygous allele. It was transmitted to progeny TOY-114M, TOY-115F, and TOY-132F. At G5, mutation #187 became homozygous in TOY138M and TOY131F, and thus were fixed in the progeny. Conversely, in another branch, the mutation was not transmitted from TOY-234M and TOY-236F (G6) to their offspring and eventually disappeared. The mutated locus is indicated in red.

had likely occurred in the germ cell lineage of the parents, because the original mutated allele was detected in multiple mice of the same generation (Fig. 3b). For three mutations on the X chromosome (Mutation ID #257, #261 and #262), which began in males with a heterozygous status (Supplementary Fig. S4 online), the mutation probably occurred in a cell at an early stage of embryonic development, resulting in mosaicism of tail tissue. These results showed that the germline mutations occurred at different developmental stages of the germ cell lineage. It is noteworthy that most germline mutations occurred during mitoses, because the germ cell lineage from fertilized egg to differentiated sperm or egg requires a large number of mitoses and only one meiosis. In the other cases (233/247) shown in Fig. 3b (G2–G8), the original mutated allele was found in a single mouse of each generation, and we could not identify when the mutation occurred.

By analogy to the *E. coli* system, we considered that 8-oxoG-induced G to T mutation is suppressed by OGG1, MUTYH, and MTH1, whereas the A to C mutation is prevented by MTH1 in mammalian cells (Supplementary Fig. S5 online). However, in contrast to the *E. coli* *mutT*, *mutM*, *mutY* triple mutant, in which both G to T and A to C mutations increased<sup>21</sup>, no A to C germline mutations were detected in the TOY-KO mouse. Thus, it is likely that different mechanisms, such as mismatch repair<sup>22</sup> or proof reading by DNA polymerase, may function to avoid A to C mutations caused by 8-oxodGTP in the TOY-KO mouse, even in the absence of MTH1. It has been reported that 2-hydroxy-deoxyadenosine (2-OHdA), an oxidized form of deoxyadenosine, is recognized as a substrate by the MUTYH protein and possesses premutagenic features<sup>23,24</sup>. 2-OHdATP, a triphosphate form of 2-OHdA, is a substrate of the MTH1 protein<sup>25</sup>. The MutY and MutT proteins of *Escherichia coli* cannot recognize 2-OHdA, in contrast to the mammalian

enzymes<sup>24,26</sup>. At the present, we cannot evaluate the contribution of 2-OHdA to the increase of germline mutation observed in TOY-KO mice, because we have not yet confirmed the accumulation of 2-OHdA in the DNA. Thus, the significance of 2-OHdA for germline mutations remains to be elucidated.

The TOY-KO mouse strain spontaneously accumulates mutations in the homozygous status. For genome-wide screening of mutants, this mouse has unique features and has the potential to take a complementary role to ENU mutagenesis<sup>27,28</sup>. The mutation is specific for G to T transversions, and occurs spontaneously and continuously in both male and female germ lineage cells of TOY-KO mice. The mutation rate of TOY-KO mice (0.2 mutation/Mb/generation, on average, in male and female) is lower than ENU-treated male gametes (1 mutation/0.42–1.82 Mb for male mouse<sup>27</sup>, 1 mutation/3.7 Mb in male rat<sup>28</sup>); however, the number of mutations carried by each TOY-KO mouse increased as the generations increased. Similar to ENU mutagenesis, phenotype-driven screening is available. Currently, the TOY-KO mouse is only available in the C57BL/6J genetic background; however, it would be a good system for large genome-wide screening of dominant mutations. Using such mutator mice with a well-controlled genetic background would permit the evaluation of the contribution of aging and the difference between spermatogenesis and oogenesis on the accumulation of germline mutations. This system also enables us to assess the genotoxic effects of chemical and environmental factors on mammalian germ lineage cells.

Although *de novo* germline mutations cause sporadic genetic diseases in humans, their occurrence is an important step for the evolution of species, as well as selection for survival. 8-oxoG, one of the causative molecules of these mutations, is endogenously produced by ROS generated from biological processes, such as oxygen respiration